General and Comparative Endocrinology 222 (2015) 158–166

Contents lists available at ScienceDirect

General and Comparative Endocrinology

journal homepage: www.elsevier.com/locate/ygcen

The secretogranin-II derived peptide secretoneurin modulates electric behavior in the weakly pulse type electric fish, *Brachyhypopomus gauderio*

Paula Pouso [a,b], Laura Quintana [b], Gabriela C. López [c], Gustavo M. Somoza [c], Ana C. Silva [b,d], Vance L. Trudeau [e,*]

[a] Depto Histología y Embriología, Facultad de Medicina, Universidad de la República, 11800 Montevideo, Uruguay
[b] Unidad Bases Neurales de la Conducta, Departamento de Neurofisiología Celular y Molecular, IIBCE, 11600 Montevideo, Uruguay
[c] Laboratorio de Ictiofisiología y Acuicultura, Instituto de Investigaciones Biotecnológicas-Instituto Tecnológico de Chascomús (IIBINTECH), Provincia de Buenos Aires, Argentina
[d] Laboratorio de Neurociencias, Facultad de Ciencias, Universidad de la República, 11400 Montevideo, Uruguay
[e] Centre for Advanced Research in Environmental Genomics, Department of Biology, University of Ottawa, Ottawa, Ontario K1N 6N5, Canada

ARTICLE INFO

Article history:
Received 19 March 2015
Revised 8 June 2015
Accepted 29 June 2015
Available online 2 July 2015

Keywords:
Secretoneurin
Pacemaker nucleus
Preoptic area
Electric organ discharge
Neuropeptide
Vasotocin

ABSTRACT

Secretoneurin (SN) in the preoptic area and pituitary of mammals and fish has a conserved close association with the vasopressin and oxytocin systems, members of a peptide family that are key in the modulation of sexual and social behaviors. Here we show the presence of SN-immunoreactive cells and projections in the brain of the electric fish, *Brachyhypopomus gauderio*. Secretoneurin colocalized with vasotocin (AVT) and isotocin in cells and fibers of the preoptic area. In the rostral *pars distalis* of the pituitary, many cells were both SN and prolactin-positive. In the hindbrain, at the level of the command nucleus of the electric behavior (pacemaker nucleus; PN), some of SN-positive fibers colocalized with AVT. We also explored the potential neuromodulatory role of SN on electric behavior, specifically on the rate of the electric organ discharge (EOD) that signals arousal, dominance and subordinate status. Each EOD is triggered by the command discharge of the PN, ultimately responsible for the basal EOD rate. SN modulated diurnal basal EOD rate in freely swimming fish in a context-dependent manner; determined by the initial value of EOD rate. In brainstem slices, SN partially mimicked the *in vivo* behavioral effects acting on PN firing rate. Taken together, our results suggest that SN may regulate electric behavior, and that its effect on EOD rate may be explained by direct action of SN at the PN level through either neuroendocrine and/or endocrine mechanisms.

1. Introduction

Vaudry and Conlon (1991) originally isolated a peptide from frog brain that Kirchmair et al. (1993) named 'secretoneurin' a few years later. The bioactive peptide SN arises from the proteolytic processing of the ~600 amino acid secretogranin-II (SgII) precursor protein by specific prohormone convertases in several tissues. In goldfish, SN-like immunoreactive (SN-ir) fibers and nerve terminals were visualized in the periventricular preoptic nucleus, pituitary and the ventrocaudal aspect of the nucleus of the lateral recess (Canosa et al., 2011). The most conspicuous SN-ir was found in the magnocellular and parvocellular cells of the preoptic nucleus that project heavily to the neural lobe of the goldfish pituitary (Canosa et al., 2011). It has been reported in goldfish and mouse that native SN peptides stimulate luteinizing hormone release *in vitro*, thus revealing a role in the control of vertebrate reproduction (Zhao et al., 2006, 2010, 2011). SN also stimulates feeding behavior in goldfish (Trudeau et al., 2012). In the rat, SN has been shown to produce increases in extracellular glutamate and GABA levels, and in central dopamine release *in vivo* (Agneter et al., 2002; You et al., 1996). Overall, these and other studies demonstrate both hormone-like and neuromodulatory effects of SN (Trudeau et al., 2012; Zhao et al., 2009).

Weakly electric fish are advantageous model systems for behavioral neuroendocrinology, including neuropeptidergic modulations of social behaviors. The electric organ discharges (EODs) displayed by South American electric fish (Order Gymnotiformes) constitute easily measurable, conspicuous, and distinctive electric behaviors that depend on well-described neural circuits (Caputi, 2005). Each EOD is triggered by the command discharge of a medullary structure, the pacemaker nucleus (PN), which is composed of two

* Corresponding author.
E-mail address: trudeauv@uottawa.ca (V.L. Trudeau).

http://dx.doi.org/10.1016/j.ygcen.2015.06.015
0016-6480/

different neuronal types: intrinsically autorhythmic pacemaker cells and projecting bulbospinal relay neurons (Bennett et al., 1967; Caputi, 2005). The PN itself commands the regular basal rhythm of the EOD, whereas modulations arise from higher centers (pre-pacemaker structures) to continuously adapt PN firing rates to environmental, physiological, and/or social contexts (Kawasaki and Heiligenberg, 1989, 1990; Keller et al., 1991; Quintana et al., 2011).

Our study species, *Brachyhypopomus gauderio* (Giora and Malabarba, 2009), modulates EOD rate in a very precise context-dependent manner. The EOD firing rate is proportional to water temperature (Silva et al., 2007). It exhibits a clear circadian cycle with nocturnal increases that are further enhanced in social interactions (Perrone et al., 2010; Silva et al., 2007), and locomotion is always associated to EOD rate increases. Novel stimuli in the surroundings produce sharp and transient increases in the EOD rate. During courtship, females and males actively communicate in a back and forth "electrical dialogue"; to inform their readiness to spawn males emit high-frequency chirps, while females interrupt their discharge intermittently (Perrone et al., 2009; Silva et al., 2008).

The arginine-vasopressin (AVP)/oxytocin (OXT) neuropeptides are major controllers of social behaviors in numerous vertebrates (Goodson and Bass, 2001; Goodson and Thompson, 2010), including humans (Ebstein et al., 2012). Arginine-vasotocin (AVT), the piscine homolog of mammalian AVP, induces a persistent increase of EOD rate, acting directly on the PN of *B. gauderio* (Perrone et al., 2010, 2014). In *B. gauderio*, AVT is responsible for the social component of the nocturnal increase of EOD rate (Perrone et al., 2010) and induces the electrical dominance observed after agonistic encounters between males (Silva et al., 2013).

The AVP and OXT neurons, located at the supraoptic and paraventricular hypothalamic nuclei of mammals, also contain and release other neuropeptides (Meister, 1993). Importantly, the neuropeptide secretoneurin (SN) is co-localized with AVT and isotocin (IST; fish homolog of tetrapod OXT) in the preoptic area (POA) and neurointermediate lobe of the goldfish pituitary (Canosa et al., 2011) and in the AVP/OXT neurons in the rat (Mahata et al., 1993). Given the importance of AVT/IST in the modulation of social behaviors (Goodson and Bass, 2001;Goodson and Thompson, 2010) and the clear effects of AVT on EOD in *B. gauderio* (Perrone et al., 2010, 2014), we have investigated the distribution and action of SN in this species.

Our ultimate goal is to explore the potential neuromodulatory role of SN on social behavior. For this purpose, in this study we first focused on the immunoidentification of SN in the brain. In addition, we evaluated the effect of SN on electric behavior using two complementary approaches: (a) *in vivo*, in which we subjected isolated and undisturbed individuals during their resting phase to SN injections, and (b) *in vitro*, in which we recorded the PN neural activity in brain slices subjected to injections of SN. This study has set the stage to analyze SN modulations in complex behavioral scenarios.

2. Materials and methods

2.1. Animals

In this study we used 34 female adult fish of *B. gauderio* (Giora and Malabarba, 2009; formerly *Brachyhypopomus pinnicaudatus*, see Hopkins, 1991), ranging from 11 to 18 cm in length and 5.5–11.2 g of body weight. Restricting this study to isolated, adult, non-breeding, female animals recorded during daytime allowed us to avoid previously described modulations of electric behavior (Perrone et al., 2009; Silva et al., 2007).

Fish were originally collected from Laguna Lavalle (31°48′S, 55°13′W, Department of Tacuarembó, Uruguay) using a "fish detector", an electronic audio amplifier connected to a pair of electrodes as previously described (Silva et al., 2003). Fish were then housed in social groups (2 males-6 females) in 500 l outdoor tanks, whose water temperature and conductivity were kept within the normal range of the natural habitat (Silva et al., 2003), and fed *ad libitum* with *Tubifex spp.* In order to achieve reliable and repeatable behaviors, our collection, trans-portation, housing, and recording conditions were adjusted in order to minimize stress. All experiments were performed in accordance with institutional and national guidelines and regula-tions for animal welfare (Comisión Honoraria Experimentación Animal, Universidad de la República, Protocol Number 008/002).

2.2. Immunohistochemistry

Fish ($n = 14$) were anesthetized by immersion in 0.05% 2-phenoxy-ethanol (Sigma, P-1126) and then perfused with saline followed by 4% paraformaldehyde in phosphate buffered saline (PBS, 25–35 ml; pH = 7.4). Brains were dissected, post-fixed overnight in the same fixative at 4 °C, and rinsed in 0.1 M PBS. Brains were embedded in gelatin/albumin and sectioned transversally (perpendicular to the longitudinal axis of the fish) on a vibrating microtome.

Vibratome sections (50–60 μm) of the brain were processed for immunohistochemical localization of SN, IST and AVT. Sections were rinsed in PBS, and non-specific binding sites were blocked with 0.5% bovine serum albumin (BSA, Sigma) for 1 h. Sections were incubated for 16 h in primary antibody dissolved in 0.1 M PBS and 0.3% Triton X-100 (PBT) with 0.5% BSA. After incubation with the primary antibody, sections were rinsed (3 × 10 min in PBS) and incubated for 2 h at room temperature with secondary antibody. All sections were then rinsed (3 × 10 min in PB), mounted in glycerol (Sigma) and cover-slipped. The following primary antibodies were used: (1) anti-goldfish SN (rabbit or mouse polyclonal; Zhao et al., 2009). These SN antisera were generated against the most conserved central portion of vertebrate SN and have been extensively validated (Canosa et al., 2011; Zhao et al., 2009). To confirm the specificity of the immunostaining, control sections were incubated with SN antisera (1:1000) pre-adsorbed overnight (4 °C) with 5 μM of synthetic goldfish SNa. (2) anti-OXT (guinea pig, polyclonal, 1:1000, cat. #T-5021, Peninsula Labs, Santa Carlos, CA, USA). This antiserum has been previously used to identify IST-positive cells in goldfish (Canosa et al., 2011). The anti-OXT antiserum (1:2500 to 1:60,000) was preabsorbed overnight (4 °C) with 10–100 μM of synthetic IST (AbD Serotec, Raleigh, NC, USA). (3) anti-AVT (rabbit, polyclonal, 1:3000, from Dr. M. Grober, Georgia State University, USA). The use of this antiserum has been previously validated for teleost fish (Perrone et al., 2014; Ramallo et al., 2012). Control sections were incubated with the primary antiserum pre-absorbed with an excess of AVT (1 μg/ml) (Cat. #66-0-09, American Peptide Company Inc., Sunny Valley, CA, USA). The following secondary antibodies were used: (1) Alexa Fluor 633 (red) goat anti-rabbit IgG (H + L) (A21070, Invitrogen, Eugene, OR, USA) for SN; (2) Alexa Fluor 633 (red) goat anti-mouse IgG (H + L) (A21050, Invitrogen) for SN; (3) Alexa Fluor488 (green) goat anti-guinea pig IgG (H + L) (A11073, Invitrogen) for IST; and (4) Alexa Fluor 488 (green) donkey anti-rabbit IgG (H + L) (A21206, Invitrogen) for AVT. The final dilutions for the secondary antibodies were 1:1000. Control experiments omitting the primary antibody were routinely performed. The CNS cytoarchitecture was identified following Maler et al. (1991).

Brains with the pituitary gland attached were fixed by submersion in Bouin's solution overnight at 4 °C. Following routine

histological procedure, the brains were dehydrated and embedded in paraffin wax and 6 μm sections were obtained and mounted on TESPA-coated slides. The next day, the sections were dewaxed, rehydrated with a serial graded of ethanol and with PBS.

To reveal the fine structure of fibers and cells in the pituitary, SN immunoreactivity was revealed with DAB (3,3′-diaminobenzidine tetrahydrochlorate hydrate). Endogenous peroxidase activity was blocked with 0.3% H_2O_2 at room temperature for 35 min. The paraffin sections were washed with PBS and incubated to blocked nonspecific binding with PBS containing 1% bovine serum albumin (BSA) and 0.3% Triton X-100 at room temperature for 35 min. Then, they were incubated with the rabbit anti-SN 1:1000 overnight at 22 °C. The next day, the sections were rinsed in PBS and immunostaining using LSAB-HRP kit (DAKO, Carpinteria, CA, USA). They were incubated with the biotinylated-secondary antibody for 35 min at room temperature and after rising with PBS, the sections were subsequently incubated with streptavidin-HRP for 35 min at room temperature to finally be washed with PBS and developed using DAB (Sigma–Aldrich). They were finally washed with distilled water, dehydrated and mounted.

Paraffin sections were also used for immunofluorescence experiments in the pituitary. After blocking non-specific binding, the sections were incubated with a mix of mouse anti-SN antiserum (1:500) and rabbit anti-chum salmon PRL antiserum (1:500, kindly provided by Dr. H. Kawauchi, Kitasato University, Japan; see Vissio et al. (1997) for methods) diluted in PBS overnight at 22 °C. The next day, sections were rinsed with PBS and incubated for 90 min with secondary antibodies (1:100, diluted in blocking solution) Alexa Fluor 594 (red) goat-antimouse IgG (HþL) (A-11076, Invitrogen,Eugene, OR) for SN, and Alexa Fluor 488 (green) goat antirabbit IgG (HþL) (A11008, Invitrogen) for PRL at 37 °C. The sections were washed twice with PBS and mounted with mounting medium with DAPI (Vector Laboratories, Inc. Burlingame, CA, USA).

2.3. Microscopy and image acquisition

Brain sections were viewed with an Olympus BX61 light microscope, with either epi-illumination or confocal microscopy (Olympus VF300). Confocal images were imported into Fluoview 5 (Olympus). The Z-stacks and orthogonal views were generated and then exported to Inkscape (0.48, Boston, MA, USA) for image adjustment. In the case of pituitary sections, the photographs were captured using a Nikon Eclipse E600 microscope with a Nikon digital imaging system. The digital images were assembled in Photoshop (Adobe Systems, San Jose, CA) adjusting only brightness, contrast, and color balance.

2.4. Behavioral experiments

Fish were placed in an experimental setup that allowed simultaneous video and electric recordings as described and validated elsewhere (Perrone et al., 2009, 2010; Silva et al., 2007). The day–night cycle and the physicochemical parameters (water temperature, conductivity, and pH) of non-breeding outdoor housing tanks were reproduced in the experimental tanks, consisting of 40 l glass aquaria (55 cm × 40 cm × 25 cm). Isolated females remained in the recording tank at constant temperature (20–22 °C) and water conductivity (150–200 μS/cm) for 12 h before the beginning of the experiment. The EODs of freely moving isolated females were detected by two pairs of orthogonal electrodes attached to each tank wall, connected to two high-input impedance amplifiers (FLA-01, Cygnus Technologies Inc.), captured by a video card (Pinnacle Systems, PCTV-HD pro stick) and stored in a computer.

As neuropeptide actions are known to be context-dependent (Goodson, 2008), we started to test the effects of SN in the most basal situation for the nocturnal gregarious species, *B. gauderio*: non-breeding isolated freely-swimming individuals during daytime (10–14 h). Goldfish type A secretoneurin (SNa, 1 μg/g bw, $n = 8$) was injected intraperitoneally (IP), following Zhao et al. (2006). Its effect on EOD rate was tested against saline-injected fish (NaCl 0.6% pH 6.4, 10 μl/g bw, $n = 6$). After 60 min of basal recording either SNa or saline was administered, and their effects were tested for 180 min. The EOD rate of 26 other non-breeding fish was similarly recorded during daytime (between 10:00–11:00 h) to quantify the range of EOD rates among individuals. To evaluate if SNa had effects on locomotor activity, we tested the frequency of the behavioral state defined as "motion" (recognized by EOD amplitude changes >20%; Perrone et al., 2010) 150–180 min after IP SNa or saline administration.

We sampled 10s-EOD recordings every 5 min, and calculated the mean EOD interval in each sample using the software Clampfit 10.0.0.61 (Axon Instruments, Foster City, CA, USA). This interval was converted to frequency and represented the EOD rate of each sample. The EOD basal rate of each fish was calculated as the median of EOD rate values of 3 samples recorded before treatment (45 min, 30 min, and 15 min before SNa administration). The EOD rate post-treatment was calculated as the median of EOD rate values of 3 samples recorded from 170 to 180 min after SN injection.

To be able to compare individuals, we evaluated the effect of the administration of SNa vs saline by quantifying the ratio of EOD rate change (rate variation index, RVI) calculated as follows: the difference between the EOD rate post-treatment and the EOD rate basal rate normalized to the EOD basal rate. RVI > 0 and RVI < 0 imply increases and decreases in EOD rate, respectively; whereas RVI = 0 means no effect on EOD rate (Perrone et al., 2010; Silva et al., 2007).

2.5. In vitro electrophysiological experiments

Adult females ($n = 6$) were chosen at random from the housing pools and anesthetized with sodium pentobarbital (Merck, 10 μl/g bw, final dose 25 μg/g bw, IP). The dorsal surface of the brain was exposed while bathed with cold sodium-free Ringer-sucrose solution (containing in mM 209 sucrose, 3 KCl, 0.75 KH_2PO_4, 1.2 $MgSO_4$, 1.6 $CaCl_2$, 24 $NaHCO_3$, and 10 D-glucose, pH = 7.4 after saturation with 95% O_2–5% CO_2). The brain with part of the spinal cord was rapidly removed from the skull and submerged in cold Ringer-sucrose solution. The entire surgical procedure took less than 5 min. Transverse sections of the brain (700 μm thick) were obtained under cold Ringer-sucrose using a vibratome (Leica, VT1000S). Slices were incubated at room temperature for 30 min in a 1:1 solution of Ringer-sucrose and fish Ringer (containing in mM, 124 NaCl, 3 KCl, 0.75 KH_2PO_4, 1.2 $MgSO_4$, 1.6 $CaCl_2$, 24 $NaHCO_3$, and 10 D-glucose, pH = 7.4 after saturation with 95% O_2–5% CO_2). Slices were then transferred to the recording chamber contain-ing fish Ringer solution. The slice containing the PN was maintained in the recording chamber and superfused with oxygenated Ringer solution at room temperature (17–22 °C) at a very slow rate of 75 μl/min. It has been already demonstrated that in these conditions, the PN maintains its spontaneous synchronized activity with a stable firing rate for several hours (Perrone et al., 2010). All the experiments were carried out during daytime.

Field potential recordings of PN activity were carried out as validated and described elsewhere (Perrone et al., 2010; Quintana et al., 2011). Briefly, recordings were performed with low resistance glass micropipettes (3–5 MΩ) filled with fish Ringer solution. The field potential reflects the synchronous activity of the neurons of the pacemaker nucleus in close proximity with the micropipette. Signals were amplified (AM Systems, M3000, filters 150–3000 Hz)

and fed to a computer for further analysis. Once the electrode was located, it remained unmoved until the end of the experiment. After recording basal activity for 30 min, 20 μl of vehicle (sterile double-distilled water) was added to an intermediate chamber, in order to test its effect on the firing rate of the PN. Two hours later, goldfish SNa (20 μl of 1 μg/μl SN; 1 μM final concentration) was added to the same intermediate chamber. All experiments were performed using the same batch of SNa.

Samples of *in vitro* electric recordings (30 s, taken every 5 min) were obtained for up to 120 min after saline injection and 200 min after SNa administra-tion. As for behavioral data, the mean PN discharge interval in each sample was calculated using the software Clampfit 10.0.0.61 (Axon Instruments, Foster City, CA, USA). This interval was converted to frequency and plotted as mean ± SD of PN discharge rate of each 30 s sample. The PN basal discharge rate of each fish was calculated as the median of the EOD rate values of the samples recorded before injection in the intermediate chamber. We evaluated the effect of the administration of SNa using the rate variation index, RVI (as described above).

2.6. Statistics

Behavioral and electrophysiological data subjected to statistical procedures are presented as median ± median absolute deviation (MAD) throughout. The non-parametric Wilcoxon matched-pairs test for paired variables was used to test the variations of EOD rate in injected fish, and Mann Whitney *U*-test was used to compare the locomotor activity between SNa-injected fish and saline controls. The relationship between RVI and EOD rate was determined by regression analysis. Statistical analysis was performed using Past 3.0 (Hammer et al., 2001).

3. Results

3.1. Secretoneurin immunoreactivity in the POA

Cells immunoreactive for SN were identified in the POA of female *B. gauderio* (Fig.1). Similar to the situation in goldfish (Canosa et al., 2011), SN-ir cells were located in rostral (Fig. 1B and C), medial (Fig. 1E and F) and caudal (Fig. 1H) sections of the POA and send their projections to the neural lobe of the pituitary gland. The distribution and size of cells resembled the parvocellular, magnocellular and gigantocellular populations of neuropeptidergic neurons of the POA. Both cytoplasm and fibers were SN-ir, while cell nuclei were not reactive (Fig. 1C, F, H). The SN antiserum produced a reaction that was completely blocked by SNa preabsorption (Fig. 1I).

Both IST and AVT were also immunohistochemically-identified in the POA (Fig. 2). The distribution of IST and AVT positive cells (shown as green fluorescence in Fig. 2) was similar to that of SN-ir cells (shown as red fluorescence in Fig. 2). As in SN-positive cells, the somata and fibers but not the nuclei were IST-ir and AVT-ir. Colocalization of SN was observed with both IST and AVT neurons and fibers (Fig. 2C, D, G, H). The colocalization of SN and IST is evident in Fig. 2C and D appearing as an orange and yellow color in the merged image and in the confocal Z-stack projection (Fig. 2D). However, some parvocellular and magnocellular elements were only SN-positive (data not shown). In some somata, one of the peptides was dominant resulting in either more greenish or reddish fluorescence (Fig. 2C). In addition, some fibers were SN positive but IST negative (Fig. 2C).These SN-ir fibers were in the proximity of somata double-labeled with anti-SN and anti-IST (Fig. 2C). The preabsortion of OXT antiserum with IST peptide (100 μM) blocked the reaction of the antibody in the tissue, and OXT-ir was not affected by preincubating the tissue with AVT (1 μg/ml) (data not shown). Some somata and fibers of SN-positive POA cells colocalize with AVT, appearing as an orange and yellow color in the merged figure (Fig. 2G) and in the confocal Z-stack projection (Fig. 2H). The colocalization of SN and AVT was identified in fibers emerging from the soma (Fig. 2G) and in distal projections (Fig. 2G inset). Nevertheless, some fibers (Fig. 2G) and somata (data not shown) were only SN positive. Preincubation of AVT antiserum with AVT peptide showed no reaction in the tissue (data not shown), and AVT immunoreactivity was not affected by preincubating the tissue with IST, demonstrating specificity of the AVT antiserum.

3.2. Secretoneurin-positive cells in the rostral pars distalis of the pituitary gland

In the pituitary gland, both SN-ir fibers and cells were detected. These cells were mainly located in rostral *pars distalis* of the pituitary (Fig. 3A). This corresponds to the area where most PRL cells are clustered in the teleost pituitary gland (Cerdá Reverter and Canosa, 2009). The double-labeling with anti-SN (in red) and anti-PRL (in green) showed that the great majority of these cells are lactotrophs expressing both, PRL and SN (Fig. 3B). A few SN-ir cells were also observed in the proximal *pars distalis* (Fig. 3A).

3.3. Secretoneurin-positive fibers reach the pacemaker nucleus

Fibers exhibiting distinct SN-ir were identified in the medulla at the level of the PN of *B. gauderio* (Fig.4C and D). The SN-ir fibers were visualized in proximity to PN neurons (Fig. 4D). As previously described in *B. gauderio* (Perrone et al., 2014), AVT-ir fibers were observed in proximity to the PN (Fig. 4G). No IST-ir fibers were observed (data not shown). In the PN sections, the SN-positive fibers were less abundant than AVT-positive fibers. Around the PN, most fibers were exclusively SN-ir (Fig. 4C and D) or AVT-ir (data not shown), whereas only a few of the SN-ir fibers colocalized with AVT (as shown in Fig. 4H).

3.4. Effects of SNa on electric behavior

Basal EOD rate exhibited a wide range of variation among individual resting *B. gauderio* recorded in social isolation, at constant temperature and water conductivity (14.1 ± 4.8 Hz (mean ± SD), range 5.3–29.2 Hz; $n = 40$). However, EOD rate was very stable in each recorded fish and remained unchanged 180 min after saline injections (pre-saline EOD rate, median ± MAD = 13.9 ± 3.9 Hz; 180 min post-saline EOD rate, median ± MAD = 13 ± 1.8 Hz, Wilcoxon matched-pairs test, $n = 6$; $p = 0.46$). After the administration of SNa: (a) 4 out of 8 fish increased their EOD rate with RVI ranging from 0.04 to 0.34 180 min after treatment (Fig. 5); (b) 4 out of 8 fish decreased their EOD rate with RVI ranging from −0.03 to −0.28 180 min after treatment (Fig. 5); and (c) there were no observable changes in locomotor activity (frequency of motion behavioral unit in saline controls versus SNa injected fish, $n_1 = 6$, $n_2 = 8$, Mann Whitney *U*-test, $p = 0.753$). In all cases, the effects on EOD rate were observed within 30 min following SNa injection and persisted for the entire recording period (180 min). Treatment with SNa increased or decreased EOD rate depending on the individuals' initial rate; i.e., in animals with a low initial EOD rate SNa induced a rate increase, whereas in animals with a high initial EOD rate SNa induced the opposite effect. Interestingly, EOD initial rate had a predictive value on RVI ($R^2 = 0.796$, $p = 0.002$; $n = 8$), indicating that both the magnitude and the polarity of the SNa effect was highly dependent on individual basal EOD rate (Fig. 5). Consequently, EOD rates observed prior to treatment ranged from 11 to 27.8 Hz. While after SNa administration this range narrowed

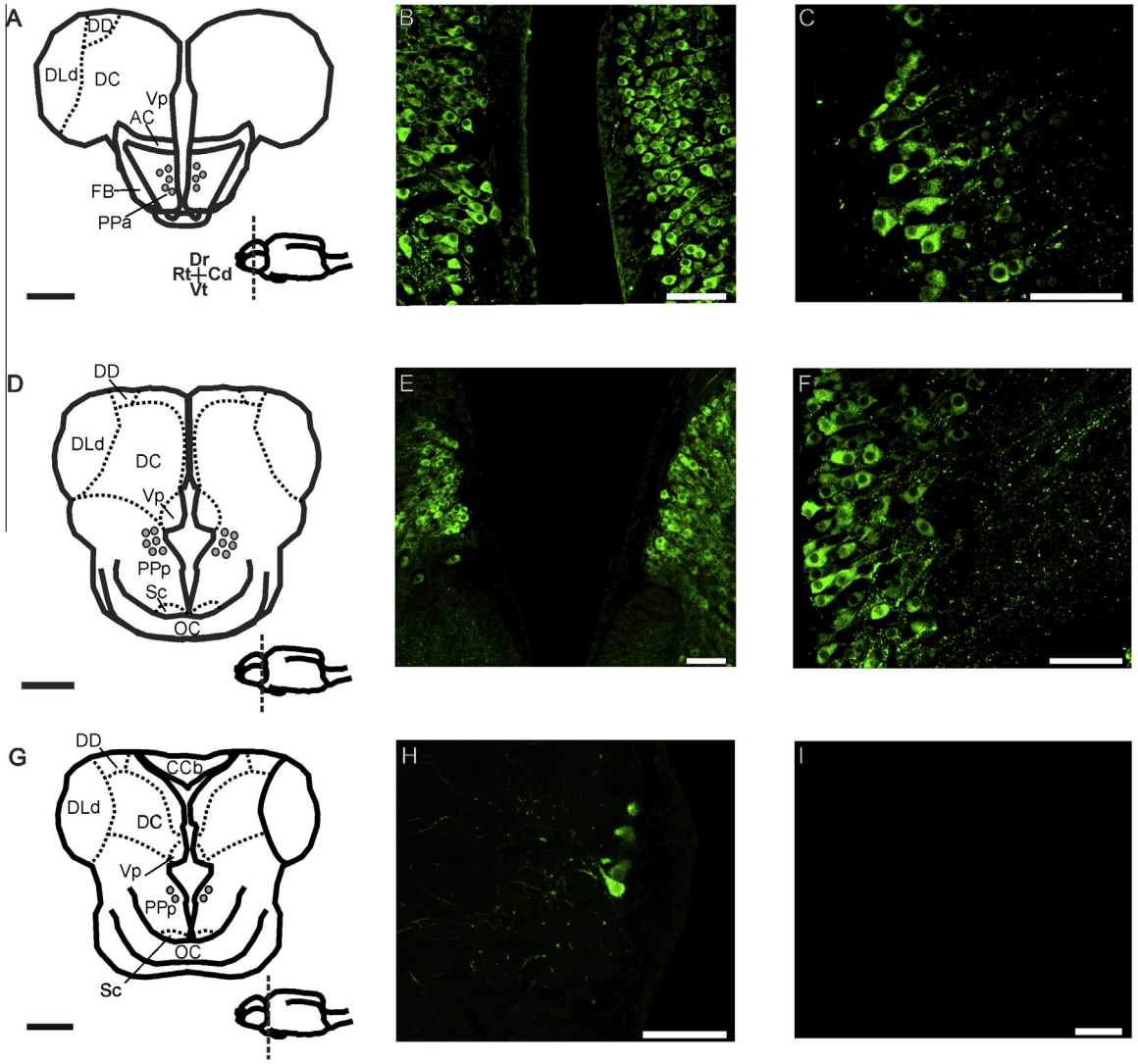

Fig. 1. Secretoneurin-like immunoreactivity (SN-ir) in transverse sections of the preoptic area (POA) of female *Brachyhypopomus gauderio*. (A) Diagram of a rostral section of the POA. The dots indicate the location of SN-ir cell bodies; (B) rostral section of the POA. Both parvocellular and magnocellular neurons are SN-ir (white); (C) magnification of an area of the tissue section shown in panel B. Both SN-ir somata and fibers are observed. (D) Diagram of a medial section of the POA. The dots indicate the location of SN-ir cell bodies. (E) Medial section of the POA. Both parvocellular and magnocellular neurons are SN-ir. (F) Magnification of an area of the tissue section shown in panel E. Both SN-ir somata and fibers are observed. (G) Diagram of a caudal transverse section of the POA. The dots indicate the location of SN-ir cell bodies. (H) Caudal section of the POA. Magnocellular neurons are SN-ir. (I) Complete inhibition of the SN immunoreaction in a rostral section of the POA after the preabsorption of the SN antiserum with SNa (5 μM). Scale bars in A, D, G: 500 μm; scale bars in B, C, E, F, H, I: 50 μm. AC, anterior commissure; CCb, corpus cerebelli; DC, central division of dorsal forebrain; DD, dorsal division of dorsal forebrain; DLd, dorsolateral telencephalon, dorsal division; FB, forebrain bundle; OC, optic chiasm; PPa, nucleus preopticus periventricularis, anterior subdivision; PPp, nucleus preopticus periventricularis, posterior subdivision; Sc, suprachiasmatic nucleus; Vp, ventral telencephalon, posterior subdivision.

to 14.7–23.6 Hz, and average values remained similar and were 17.9 and 17.6 pre- and post-treatment, respectively.

The PN had a low firing rate with very little variability when isolated in the slice and kept in stable chamber conditions *in vitro* (10.4 ± 1.9 Hz, range 6.8–13.7 Hz; $n = 12$). Perfusion of the preparation with the vehicle had no effect on the PN discharge rate (Fig. 6). Pre-vehicle PN rate (median ± MAD) was 9.8 ± 1.2 Hz while 120 min post-vehicle PN rate (median ± MAD) was 10.1 ± 1.1 Hz (Wilcoxon matched-pairs test, $n = 6$, $p = 1$). The perfusion with SNa (1 μM) produced an increase in 3 out of 6 cases, which had very low initial basal rates ranging from 6.8 to 10.4 Hz. In these cases, the effect on PN firing rate could be observed 90 min after SNa administration and persisted for at least 180 min with RVIs ranging from 0.13 to 0.53 (Fig. 6). In the other 3 cases, which had higher initial basal rates ranging from 9.5 to 13.7 Hz, we observed no changes in PN firing rate after perfusion with SNa *in vitro*. In these cases, PN rates remained stable throughout the experiments, with RVIs ranging from −0.08 to −0.03 (Fig. 6).

4. Discussion

Secretoneurin, an evolutionarily conserved peptide, has numerous functions that include neuroinflammation, neurotransmitter release, and neuroendocrine regulation (Trudeau et al., 2012). Interestingly, SN in the POA of mammals and fish has been shown to have a conserved close association to the AVP/OXT system (Canosa et al., 2011), a peptide family which is key in the modulation of sexual and social behaviors (Goodson and Bass, 2001; Goodson and Thompson, 2010). In this study we have shown that in the *B. gauderio*, SN is produced by preoptic neurons and endocrine cells of the pituitary, and that its distribution reaches the hindbrain, in the vicinity of the PN. This is the first report to show

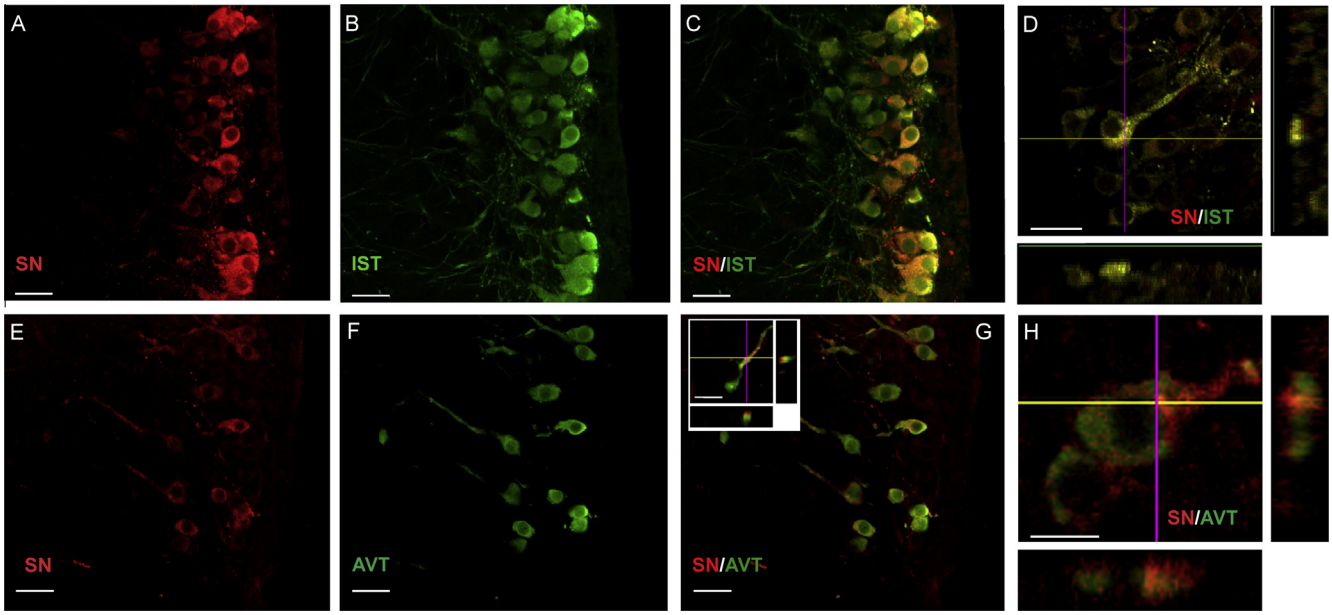

Fig. 2. Colocalization of secretoneurin-like immunoreactivity (SN-ir) with isotocin (IST) and arginine vasotocin (AVT) in medial transverse sections of preoptic area (POA) of female *Brachyhypopomus gauderio*. (A) SN-ir somata (red). (B) IST-ir somata (green). (C) Colocalization of SN-ir and IST-ir is shown as an orange to yellow color in somata and fibers. (D) Colocalization of SN and IST in a magnocellular neuron, Z-stack projection and orthogonal view. (E) SN-ir somata (red). (F) AVT-ir somata (green). (G) Colocalization of SN-ir and AVT-ir is shown as an orange to yellow color in somata and fibers. (G, inset) Detail of a fiber double-labeled with SN and AVT. Z-stack projection and orthogonal view. (H) Colocalization of SN and AVT in a magnocellular neuron. Z-stack and orthogonal view. Scale bars: A–G: 20 μm; I inset, H inset: 10 μm. (For interpretation of the references to colour in this figure legend, the reader is referred to the web version of this article.)

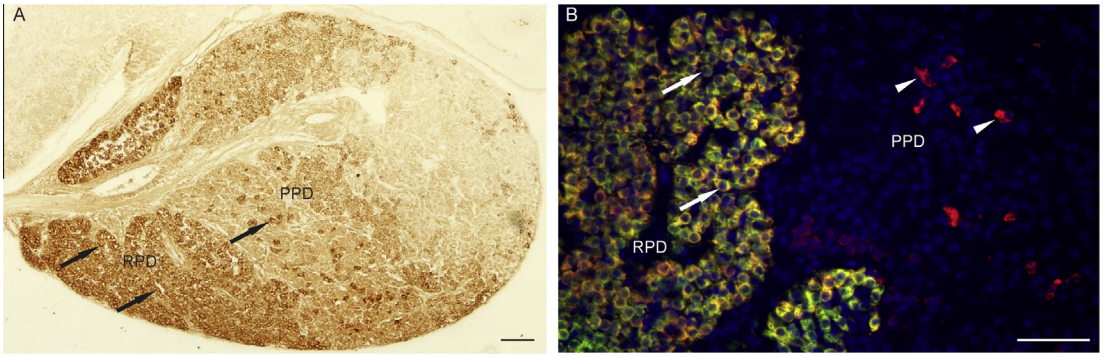

Fig. 3. (A) Sagittal view of *Brachyhypopomus gauderio* pituitary gland. Secretoneurin-immunoreactive (SN-ir; brown shows the DAB (3,3′-diaminobenzidine tetrahydrochlorate hydrate reaction) cells are shown in the rostral *pars distalis* surrounding nerve terminals entering the pituitary gland (arrows). Some SN-ir cells can be seen isolated in the proximal *pars distalis* (arrows). (B) Colocalization of secretoneurin (SN) and prolactin (PRL) in the *Brachyhypopomus gauderio* pituitary gland. Most of the cells in the rostral *pars distalis* are also immunoreactive for both SN (red) and PRL (green) resulting in a yellowish coloration (full arrows). Some dispersed SN-ir cells (red) were also detected at the proximal *pars distalis* (arrowheads). The blue reaction represents the nuclear stain DAPI. Scale bars: A: 100 μm; B: 20 μm. RPD, rostral *pars distalis*; PPD, proximal *pars distalis*. (For interpretation of the references to colour in this figure legend, the reader is referred to the web version of this article.)

the influence of SN on electric behavior, and among the few studies that have considered the neuromodulatory effect of SN on behavior. Secretoneurin modulates the diurnal basal EOD rate, exerting at least part of its effects on EOD rate directly at the PN level and in a context-dependent manner.

4.1. SN cells and projections

Immunostaining was performed with an antibody generated against the central core of the most conserved portion of vertebrate SN peptide. This antiserum revealed clearly labeled cell bodies and fibers throughout the POA, with a distinct location in the parvocellular, magnocellular and gigantocellular neuronal populations, in agreement with reports for this and other neuropeptides (Canosa et al., 2011; Greenwood et al., 2008; Larson et al., 2006). Secretoneurin-ir was also localized in endocrine cells of the pituitary *pars distalis*, and the terminal nerves that form the *pars nervosa*. Furthermore, projections of SN neurons were labeled in the hindbrain, in close vicinity to the PN, which commands the rhythm of the EOD. This description of SN distribution, particularly in nerve terminals in the posterior pituitary, endocrine cells of the *pars distalis* and in fibers in and around the PN raise the distinct possibility that SN may be exerting a regulating influence by both endocrine and/or neuroendocrine mechanisms.

In the POA prominent SN-ir in perikarya and fibers colocalized with both AVT and IST. This included the innervation of the *pars nervosa* of the pituitary where AVT, IST and presumably SN are released from nerve terminals. This colocalization is consistent with what is known about SN-ir in goldfish, the only other teleost where SN distribution has been evaluated, and reinforces the notion that SN may well be involved in the AVT/IST modulation of sexual, aggressive and/or affiliative behaviors. Additionally,

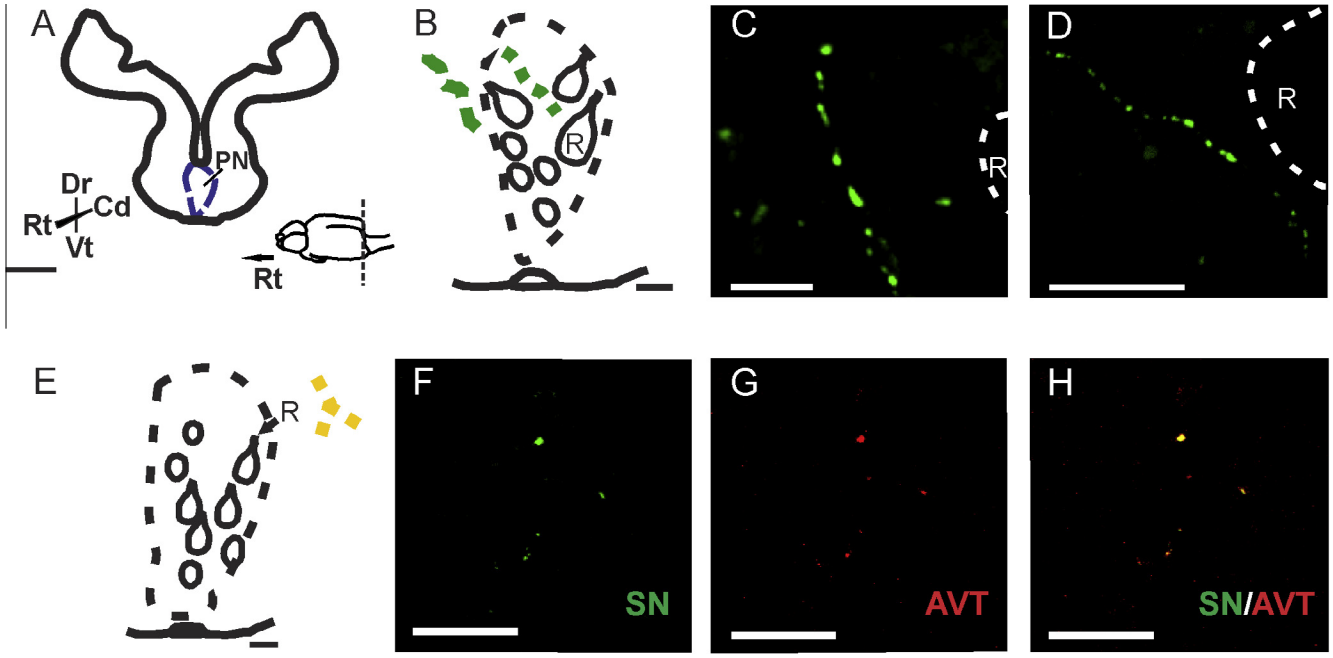

Fig. 4. Secretoneurin-immunoreactive (SN-ir) fibers in the proximity of the pacemaker nucleus (PN). (A) Diagram of a transverse section of the medulla at the level of the PN. The border of the PN is shown in blue. (B) Diagram of an enlarged transverse section of the PN. The green dotted lines indicate SN-ir fibers. (C and D) SN-ir fibers (green) proximate to relay neurons. (E) Diagram of a transverse section of the PN. The yellow dots indicate a fiber double-labeled for SN and AVT. (F) SN-ir fiber (green). (G) AVT-ir fiber (red). (H) Colocalization (yellow) of SN-ir and AVT-ir in a fiber. Scale bars: A: 500 μm; B, E: 50 μm; C, F, G, H: 10 μm; D: 20 μm. Dr, dorsal; Vt, ventral; Rt, rostral; Cd, caudal; R, relay neuron. (For interpretation of the references to colour in this figure legend, the reader is referred to the web version of this article.)

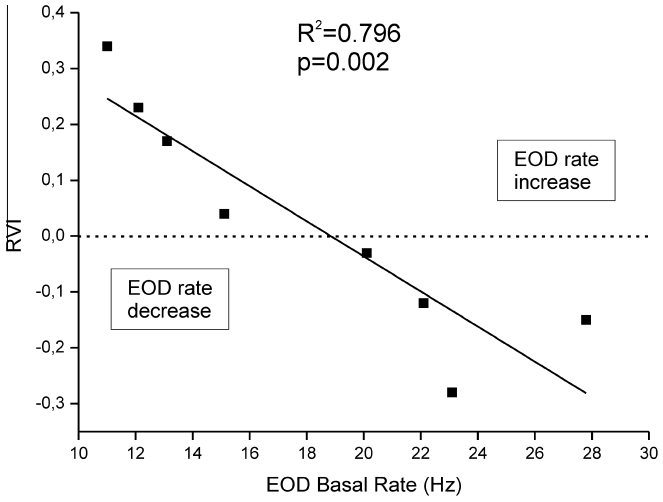

Fig. 5. The magnitude and polarity of the effect of goldfish SNa on *in vivo* basal EOD rate depends on its initial value. The dash line represents no variation in EOD rate (rate variation index, RVI = 0). Intraperitoneal administration of SNa (1 μg/g) induces either an increase in EOD rate (RVI > 0) or a decrease in EOD rate (RVI < 0). In individuals whose initial basal EOD rates were low (<15 Hz), SNa induces an increase; in individuals whose initial basal EOD rates were high (>20 Hz), SNa induces a decrease. Linear regression analysis indicates a strong negative relationship between RVI and basal EOD rate (n = 8).

SN-ir was localized to lactotrophs in the rostral *pars distalis*. This is also in agreement with observations in goldfish (Zhao et al., 2009). In addition, some SN-ir cells were also detected in the proximal *pars distalis* of *B. gauderio* corresponding to the area where growth hormone (GH) producing cells are located (Vissio et al., 1997; Sciara et al., 2006). This observation together with the previous identification of SN-ir in the goldfish pituitary gland (Zhao et al., 2009), suggests that some of these cells are likely somatotrophs.

Neuropeptidergic modulation of behavior has already been described in *B. gauderio*. It is also known that the electric behavior is affected by AVT, which induces strong EOD rate increases in this species. The PN itself appears to be the effector of this modulatory input: AVT-ir fibers lie in close proximity to the PN, and it is possible to reproduce the behavioral temporal pattern of AVT-mediated effects on EOD rate in an PN isolated preparation (Perrone et al., 2010, 2014). In this study, we found fibers around the PN that were exclusively SN or AVT-positive, and some fibers where both SN and AVT were colocalized. It has been proposed that the pattern-generating circuit of the electromotor system originates from the same genetically specified compartments of the embryonic hindbrain that gives rise to rhythmically active cardiac and respiratory circuits in vertebrates (Bass and Baker, 1997). In mammals, the nucleus of the solitary tract (NTS), a brainstem central pattern generator like the PN of weakly electric fish, is also involved in nutrient sensing and food intake. Interestingly, in the rat, the NTS presents a high density of SN fibers (Marksteiner et al., 1993) and AVP fibers (Michelini, 1998), thereby implicating SN and AVP in the modulation of respiratory rhythms and feeding. In goldfish, SNa injection into the third ventricle stimulates feeding behavior (Trudeau et al., 2012). On the whole, our results suggest that SN effects on EOD rhythms are carried out directly at the PN level through a neural influence, and perhaps through an endocrine mechanism. Future studies will be focused on the effect of both AVT and SN on PN rate, in order to understand if and how these two modulatory systems interact.

4.2. SNa modulation of electric behavior

This is the first study to demonstrate the effect of SN on an electric behavior and to identify a target of its action, the PN, which is ultimately responsible for EOD rate. The rhythm of the EOD can be considered itself an electric behavior as it signals arousal, sexual, and dominance-subordinate status (Hagedorn and Heiligenberg,

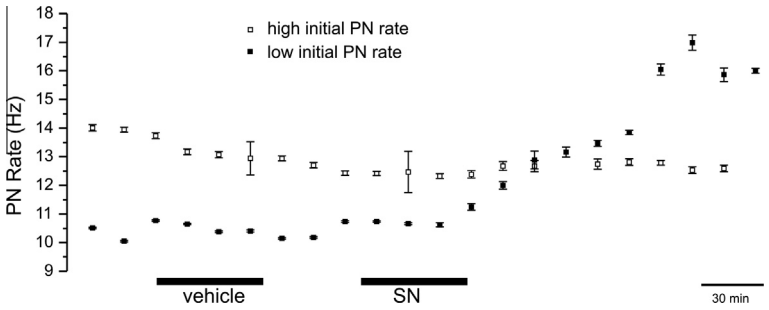

Fig. 6. Effect of goldfish SNa on *in vitro* firing rate in isolated brain slices containing the pacemaker nucleus (PN). Application of 1 μM SNa produced a delayed and persistent increase in firing rate (solid symbols) in a preparation with an initial basal rate of 10.3 Hz. On the other hand, in a preparation with an initial PN firing rate of 13.7 Hz, SNa exerted no effect, and basal firing rate remained stable throughout the recording (open symbols). Application of control vehicle (double-distilled water) had no effect on PN rate. Each symbol represents the mean ± SD instantaneous frequency of a 30 s sample of PN activity (PN field potentials).

1985; Silva et al., 2002, 2007, 2013). Following previous studies (Perrone et al., 2010, 2014; Silva et al., 2007) and to favor the link between behavior and PN physiology, we focused on the basic unit of electric behavior: the resting diurnal EOD rate of isolated individuals. Furthermore, in order to avoid the bias of sexual and reproductive modulation of electric behavior, we chose to restrict our work to non-breeding females.

Secretoneurin modulates diurnal basal EOD rate in a context-dependent manner, i.e., the magnitude and polarity of the effects of SNa depended on the initial value of EOD rate. Context-dependent effects of neuropeptides to modulate physiology and behavior are not without precedent. The effects of neuropeptide *Y* to either enhance or suppress pituitary luteinizing hormone release are context-dependent, varying according to stage of the rat estrous cycle and steroidal treatments (e.g., Knox et al., 1995). Another example demonstrates clear context-specific effects of neuropeptides to regulate behavior. Bredewold et al. (2014) demonstrated that both AVP and OXT systems in the lateral septum modulate social play in juvenile rats in neuropeptide-, sex- and social context-specific ways. Furthermore, neuropeptides can directly modulate neuronal firing patterns in state-dependent manners. For example, *in vitro*, thalamic paraventricular nucleus neurons respond to exogenously applied AVP (Zhang et al., 2006) and orexins (Kolaj et al., 2007) with membrane depolarization and state-dependent modulation of their firing patterns. Furthermore, in the agonistic behavior of the highly territorial weakly electric fish, *Gymnotus omarorum*, AVT acts differently on potential dominants depending on the size of the contended territory (R. Perrone, personal communication). Therefore, the effect of IP-injected SNa to either increase or decrease EOD firing rates may be another example of context-dependent effects of a neuropeptide.

Interestingly, we found a wide range of diurnal basal EOD rates in isolated individuals recorded at constant temperature. The emissions of EODs, which are energetically expensive signals (Crampton, 1998; Salazar and Stoddard, 2008), play dual key roles in perception and communication. In this scenario, SN may act as a homeostatic neuromodulator, involved in the complex adjustment of EOD rate as the animal copes with different contextual demands (environmental, social and physiological). Also interestingly, PN firing rates recorded *in vitro* were lower and exhibited a narrower range than *in vivo* EOD basal rates (6.8–13.7 Hz). This suggests that the isolation of the PN in the brainstem slice excludes the action of excitatory central inputs, most likely glutamatergic inputs from prepacemaker areas that are important in setting EOD rate *in vivo* (Juranek and Metzner, 1997, 1998; Kawasaki and Heiligenberg, 1988, 1989, 1990; Kawasaki et al., 1988; Keller et al., 1991; Metzner, 1993; Spiro et al., 1994).

In vivo effects of SNa on EOD rate were paralleled by the effect of SNa on PN firing rate in brainstem slices in at least two aspects. Firstly, when the initial PN firing rate was low (<10 Hz), SNa induced a long-lasting acceleration similar in magnitude and timing to the EOD rate increase observed after IP SNa administration *in vivo*. Similarly to previous data on AVT effects on electric behavior (Perrone et al., 2010, 2014), our results suggest that SNa is exerting its effects directly on the PN, most likely on the pacemaker cell population, and that, in addition to possible endocrine actions, the SN fibers identified close to the PN might be the anatomical substrate for SN influences on PN activity. Secondly, the effects of SNa on PN firing rate also depended on its initial value; but in contrast to the *in vivo* data in which SNa induced a decrease in EOD rate when the initial values were high, SNa failed to induce an effect in PN firing rate when its initial value was above 10 Hz. Different targets of SNa within the brain may explain context-dependent actions of SNa *in vivo*. The PN itself might be a target for SNa excitatory effects that were therefore retrievable in the *in vitro* preparation in which PN firing rates are always low. On the other hand, pre-pacemaker structures might be the target for SNa inhibitory effects, impossible to observe in the brainstem slice used, obviously disconnected from higher influences. Future experiments will aim to artificially increase PN firing rate in the brainstem slice (by AVT administration, for example), and then test if SNa is able to reduce PN firing rate. This will elucidate if behavioral actions of SN can be fully explained at the PN level.

From a more integrative neuroendocrine perspective our data suggest a distinct interplay of AVT and SN peptides in the modulation of electric behavior. Arginine vasotocin always induces a sudden and permanent increase in EOD rate regardless of its initial value, sex or season that can be fully explained by its action on the PN (Perrone et al., 2010, 2014). In contrast, SN induces changes in EOD rate that depend on its initial value, and that cannot be fully mimicked at the PN level. Interestingly, this fine-tuning of electric behavior, that can be already identifiable in isolated individuals, may constitute an important element of the neuroendocrine mechanisms controlling complex social interactions.

Acknowledgments

We are especially grateful to Hiroshi Kawauchi (Kitasato University) who kindly donated the anti PRL antiserum, as well as Ruud Buijs (Universidad Autónoma de Mexico) and Matthew Grober (Georgia State University) who kindly donated the AVT antibody developed in their labs. Alejandro de Lorenzi and Matías Pandolfi (Universidad de Buenos Aires) also kindly provided several of the antibodies used in this study. This research was supported by PICT2008-1383 ANPCyT, Argentina (GMS), NSERC Discovery Program and University of Ottawa Research Chair in Neuroendocrinology (VLT), CSIC UdelaR (I+D 2010_032, Uruguay), and PEDECIBA (Uruguay).

References

Agneter, E., Sitte, H.H., Stöckl-Hiesleitner, S., Fischer-Colbrie, R., Winkler, H., Singer, E.A., 2002. Sustained dopamine release induced by secretoneurin in the striatum of the rat: a microdialysis study. J. Neurochem. 65, 622–625.

Bass, A.H., Baker, R., 1997. Phenotypic specification of hindbrain rhombomeres and the origins of rhythmic circuits in vertebrates. Brain Behav. Evol. 50, 3–16.

Bennett, M.V., Pappas, G.D., Aljure, E., Nakajima, Y., 1967. Physiology and ultrastructure of electrotonic junctions. II. Spinal and medullary electromotor nuclei in mormyrid fish. J. Neurophysiol. 30, 180–208.

Bredewold, R., Smith, C.J.W., Dumais, K.M., Veenema, A.H., 2014. Sex-specific modulation of juvenile social play behavior by vasopressin and oxytocin depends on social context. Front. Behav. Neurosci. 8, 216.

Canosa, L.F., Lopez, G.C., Scharrig, E., Lesaux-Farmer, K., Somoza, G.M., Kah, O., Trudeau, V.L., 2011. Forebrain mapping of secretoneurin-like immunoreactivity and its colocalization with isotocin in the preoptic nucleus and pituitary gland of goldfish. J. Comp. Neurol. 519, 3748–3765.

Caputi, A.A., 2005. Electric organs and their control. In: Bullock, T.H., Hopkins, C.D., Popper, A.N. (Eds.), Electroreception. Springer, pp. 410–451.

Cerdá Reverter, J., Canosa, L., 2009. Neuroendocrine systems of the fish brain. In: Bernier, N.J., Van der Kraak, G., Farrell, A.P., Brauner, C.J. (Eds.), Fish Neuroendocrinology. Elsevier Inc., pp. 3–74.

Crampton, W.G.R., 1998. Effects of anoxia on the distribution, respiratory strategies and electric signal diversity of gymnotiform fishes. J. Fish Biol. 53A, 307–330.

Ebstein, R.P., Knafo, A., Mankuta, D., Chew, S.H., Lai, P.S., 2012. The contributions of oxytocin and vasopressin pathway genes to human behavior. Horm. Behav. 61, 359–379.

Giora, J., Malabarba, L., 2009. *Brachyhypopomus gauderio*, new species, a new example of underestimated species diversity of electric fishes in the southern South America (Gymnotiformes: Hypopomidae). Zootaxa 2093, 60–68.

Goodson, J.L., 2008. Nonapeptides and the evolutionary patterning of sociality. Prog. Brain Res. 170, 3–15.

Goodson, J.L., Bass, A.H., 2001. Social behavior functions and related anatomical characteristics of vasotocin/vasopressin systems in vertebrates. Brain Res. Brain Res. Rev. 35, 246–265.

Goodson, J.L., Thompson, R.R., 2010. Nonapeptide mechanisms of social cognition, behavior and species-specific social systems. Curr. Opin. Neurobiol. 20, 784–794.

Greenwood, A.K., Wark, A.R., Fernald, R.D., Hofmann, H.A., 2008. Expression of arginine vasotocin in distinct preoptic regions is associated with dominant and subordinate behaviour in an African cichlid fish. Proc. Biol. Sci. 275, 2393–2402.

Hagedorn, M., Heiligenberg, W., 1985. Court and spark: electric signals in the courtship and mating of gymnotoid fish. Anim. Behav. 33, 254–265.

Hammer, Ø., Harper, D., Ryan, P., 2001. PAST: paleontological statistics software package for education and data analysis. Paleontol. Electron. 4, 1–9.

Hopkins, C., 1991. *Hypopomus pinnicaudatus* (Hypopomidae), a new species of gymnotiform fish from French Guiana. Copeia, 151–161.

Juranek, J., Metzner, W., 1997. Cellular characterization of synaptic modulations of a neuronal oscillator in electric fish. J. Comp. Physiol. A 181, 393–414.

Juranek, J., Metzner, W., 1998. Segregation of behavior-specific synaptic inputs to a vertebrate neuronal oscillator. J. Neurosci. 18, 9010–9019.

Kawasaki, M., Heiligenberg, W., 1988. Individual prepacemaker neurons can modulate the pacemaker cycle of the gymnotiform electric fish, Eigenmannia. J. Comp. Physiol. A 162, 13–21.

Kawasaki, M., Heiligenberg, W., 1989. Distinct mechanisms of modulation in a neuronal oscillator generate different social signals in the electric fish *Hypopomus*. J. Comp. Physiol. A 165, 731–741.

Kawasaki, M., Heiligenberg, W., 1990. Different classes of glutamate receptors and GABA mediate distinct modulations of a neuronal oscillator, the medullary pacemaker of a gymnotiform electric fish. J. Neurosci. 10, 3896–3904.

Kawasaki, M., Maler, L., Rose, G., Heiligenberg, W., 1988. Anatomical and functional organization of the prepacemaker nucleus in gymnotiform electric fish: the accommodation of two behaviors in one nucleus. J. Comp. Neurol. 276, 113–131.

Keller, C.H., Kawasaki, M., Heiligenberg, W., 1991. The control of pacemaker modulations for social communication in the weakly electric fish Sternopygus. J. Comp. Physiol. A 169, 441–450.

Kirchmair, R., Hogue-Angeletti, R., Gutierrez, J., Fischer-Colbrie, R., Winkler, H., 1993. Secretoneurin – a neuropeptide generated in brain, adrenal medulla and other endocrine tissues by proteolytic processing of secretogranin II (chromogranin C). Neuroscience 53, 359–365.

Knox, K.L., Bauer-Dantoin, A.C., Levine, J.E., Schwartz, N.B., 1995. Unmasking of neuropeptide-Y inhibitory effects on in vitro gonadotropin secretion from pituitaries of metestrous, but not proestrous, rats. Endocrinology 136, 187–194.

Kolaj, M., Doroshenko, P., Yan Cao, X., Coderre, E., Renaud, L.P., 2007. Orexin-induced modulation of state-dependent intrinsic properties in thalamic paraventricular nucleus neurons attenuates action potential patterning and frequency. Neuroscience 147, 1066–1075.

Larson, E.T., O'Malley, D.M., Melloni, R.H., 2006. Aggression and vasotocin are associated with dominant-subordinate relationships in zebrafish. Behav. Brain Res. 167, 94–102.

Mahata, S.K., Mahata, M., Hörtnag, H., Fischer-Colbrie, R., Steiner, H.J., Dietze, O., Winkler, H., 1993. Concomitant changes of messenger ribonucleic acid levels of secretogranin II, VGF, vasopressin and oxytocin in the paraventricular nucleus of rats after adrenalectomy and during lactation. J. Neuroendocrinol. 5, 323–330.

Maler, L., Sas, E., Johnston, S., Ellis, W., 1991. An atlas of the brain of the electric fish *Apteronotus leptorhynchus*. J. Chem. Neuroanat. 4, 1–38.

Marksteiner, J., Kirchmair, R., Mahata, S.K., Mahata, M., Fischer-Colbrie, R., Hogue-Angeletti, R., Saria, A., Winkler, H., 1993. Distribution of secretoneurin, a peptide derived from secretogranin II, in rat brain: an immunocytochemical and radioimmunological study. Neuroscience 54, 923–944.

Meister, B., 1993. Gene expression and chemical diversity in hypothalamic neurosecretory neurons. Mol. Neurobiol. 7, 87–110.

Metzner, W., 1993. The jamming avoidance response in *Eigenmannia* is controlled by two separate motor pathways. J. Neurosci. 13, 1862–1878.

Michelini, L.C., 1998. Vasopressin in the nucleus tractus solitarius: a modulator of baroreceptor reflex control of heart rate. Braz. J. Med. Biol. Res. 27, 1017–1032.

Perrone, R., Batista, G., Lorenzo, D., Macadar, O., Silva, A., 2010. Vasotocin actions on electric behavior: interspecific, seasonal, and social context-dependent differences. Front. Behav. Neurosci. 4, 52.

Perrone, R., Macadar, O., Silva, A., 2009. Social electric signals in freely moving dyads of *Brachyhypopomus pinnicaudatus*. J. Comp. Physiol. A 195, 501–514.

Perrone, R., Migliaro, A., Comas, V., Quintana, L., Borde, M., Silva, A., 2014. Local vasotocin modulation of the pacemaker nucleus resembles distinct electric behaviors in two species of weakly electric fish. J. Physiol. Paris 108, 203–212.

Quintana, L., Sierra, F., Silva, A., Macadar, O., 2011. A central pacemaker that underlies the production of seasonal and sexually dimorphic social signals: functional aspects revealed by glutamate stimulation. J. Comp. Physiol. A 197, 211–225.

Ramallo, M.R., Grober, M., Cánepa, M.M., Morandini, L., Pandolfi, M., 2012. Arginine-vasotocin expression and participation in reproduction and social behavior in males of the cichlid fish cichlasoma dimerus. Gen. Comp. Endocrinol. 179, 221–231.

Salazar, V.L., Stoddard, P.K., 2008. Sex differences in energetic costs explain sexual dimorphism in the circadian rhythm modulation of the electrocommunication signal of the gymnotiform fish *Brachyhypopomus pinnicaudatus*. J. Exp. Biol. 211, 1012–1020.

Sciara, A.A., Rubiolo, J.A., Somoza, G.M., Arranz, S.E., 2006. Molecular cloning, expression and immunological characterization of pejerrey *(Odontesthes bonariensis)* growth hormone. Comp. Biochem. Physiol. C Toxicol. Pharmacol. 142, 284–292.

Silva, A., Perrone, R., Macadar, O., 2007. Environmental, seasonal, and social modulations of basal activity in a weakly electric fish. Physiol. Behav. 90, 525–536.

Silva, A., Quintana, L., Ardanaz, J.L., Macadar, O., 2002. Environmental and hormonal influences upon EOD waveform in gymnotiform pulse fish. J. Physiol. Paris 96, 473–484.

Silva, A., Quintana, L., Galeano, M., Errandonea, P., 2003. Biogeography and breeding in gymnotiformes from Uruguay. Environ. Biol. Fishes 66, 329–338.

Silva, A., Quintana, L., Perrone, R., Sierra, F., 2008. Sexual and seasonal plasticity in the emission of social electric signals. Behavioral approach and neural bases. J. Physiol. Paris 102, 272–278.

Silva, A.C., Perrone, R., Zubizarreta, L., Batista, G., Stoddard, P.K., 2013. Neuromodulation of the agonistic behavior in two species of weakly electric fish that display different types of aggression. J. Exp. Biol. 216, 2412–2420.

Spiro, J., Brose, N., Heinemann, S., Heiligenberg, W., 1994. Immunolocalization of NMDA receptors in the central nervous system of weakly electric fish: functional implications for the modulation of a neuronal oscillator. J. Neurosci. 14, 6289–6299.

Trudeau, V.L., Martyniuk, C.J., Zhao, E., Hu, H., Volkoff, H., Decatur, W.A., Basak, A., 2012. Is secretoneurin a new hormone? Gen. Comp. Endocrinol. 175, 10–18.

Vaudry, H., Conlon, J.M., 1991. Identification of a peptide arising from the specific post-translation processing of secretogranin II. FEBS Lett. 284, 31–33.

Vissio, P.G., Somoza, G.M., Maggese, M.C., Paz, D.A., Strüssmann, C.A., 1997. Structure and cell type distribution in the pituitary gland of pejerrey *Odontesthes bonariensis*. Fish. Sci. 63, 64–68.

You, Z.-B., Terenius, L., Saria, A., Fischer-Colbrie, R., Goiny, M., Herrera-Marschitz, M., 1996. Effects of secretogranin II-derived peptides on the release of neurotransmitters monitored in the basal ganglia of the rat with in vivo microdialysis. Naunyn. Schmiedebergs. Arch. Pharmacol. 354, 717–724.

Zhang, L., Doroshenko, P., Cao, X.Y., Irfan, N., Coderre, E., Kolaj, M., Renaud, L.P., 2006. Vasopressin induces depolarization and state-dependent firing patterns in rat thalamic paraventricular nucleus neurons in vitro. Am. J. Physiol. Regul. Integr. Comp. Physiol. 290, R1226–R1232.

Zhao, E., Basak, A., Wong, A.O.L., Ko, W., Chen, A., López, G.C., Grey, C.L., Canosa, L.F., Somoza, G.M., Chang, J.P., Trudeau, V.L., 2009. The secretogranin II-derived peptide secretoneurin stimulates luteinizing hormone secretion from gonadotrophs. Endocrinology 150, 2273–2282.

Zhao, E., Basak, A., Trudeau, V.L., 2006. Secretoneurin stimulates goldfish pituitary luteinizing hormone production. Neuropeptides 40, 275–282.

Zhao, E., Grey, C.L., Zhang, D., Mennigen, J.A., Basak, A., Chang, J.P., Trudeau, V.L., 2010. Secretoneurin is a potential paracrine factor from lactotrophs stimulating gonadotropin release in the goldfish pituitary. Am. J. Physiol. Regul. Integr. Comp. Physiol. 299, R1290–R1297.

Zhao, E., McNeilly, J.R., McNeilly, A.S., Fischer-Colbrie, R., Basak, A., Seong, J.Y., Trudeau, V.L., 2011. Secretoneurin stimulates the production and release of luteinizing hormone in mouse L(beta)T2 gonadotropin cells. Am. J. Physiol. Endocrinol. Metab. 301, E288–E297.